

Article

Influence of Settlement on Base Resistance of Long Piles in Soft Soil—Field and Machine Learning Assessments

Thanh T. Nguyen ^{1,*} , Viet D. Le ², Thien Q. Huynh ¹ and Nhu H.T. Nguyen ³

¹ School of Civil and Environmental Engineering, Ultimo Campus, University of Technology Sydney, Ultimo, NSW 2007, Australia

² Department of Civil Engineering, Gumi Campus, Kumoh National Institute of Technology, Gumi 39177, Gyeongbuk, Republic of Korea; vietld@kumoh.ac.kr

³ School of Engineering, Geelong Waurn Ponds Campus, Deakin University, Geelong, VIC 3217, Australia; nhu.nguyen@deakin.edu.au

* Correspondence: thanh.nguyen-4@uts.edu.au

Abstract: Understanding the role that settlement can have on the base resistance of piles is a crucial matter in the design and safety control of deep foundations under various buildings and infrastructure, especially for long to super-long piles (60–90 m length) in soft soil. This paper presents a novel assessment of this issue by applying explainable machine learning (ML) techniques to a robust database (1131 datapoints) of fully instrumented pile tests across 37 real-life projects in the Mekong Delta. The analysis of data based on conventional methods shows distinct responses of long piles to rising settlement, as compared to short piles. The base resistance can rapidly develop at a small settlement threshold (0.015–0.03% of pile’s length) and contribute up to 50–55% of the total bearing capacity in short piles, but it slowly rises over a wide range of settlement to only 20–25% in long piles due to considerable loss of settlement impact over the depth. Furthermore, by leveraging the advantages of ML methods, the results significantly enhance our understanding of the settlement–base resistance relationship through explainable computations. The ML-based prediction method is compared with popular practice codes for pile foundations, further attesting to the high accuracy and reliability of the newly established model.

Keywords: base resistance; pile foundation; machine learning; pile load tests; pile settlement



Citation: Nguyen, T.T.; Le, V.D.; Huynh, T.Q.; Nguyen, N.H.T. Influence of Settlement on Base Resistance of Long Piles in Soft Soil—Field and Machine Learning Assessments. *Geotechnics* **2024**, *4*, 447–469. <https://doi.org/10.3390/geotechnics4020025>

Academic Editor: Raffaele Di Laora

Received: 1 April 2024

Revised: 28 April 2024

Accepted: 29 April 2024

Published: 3 May 2024



Copyright: © 2024 by the authors. Licensee MDPI, Basel, Switzerland. This article is an open access article distributed under the terms and conditions of the Creative Commons Attribution (CC BY) license (<https://creativecommons.org/licenses/by/4.0/>).

1. Introduction

Pile foundation is one of the most reliable and effective solutions for various buildings and infrastructure, including offshore, energy and transportation, around the world [1–5]. In essence, the contribution of base resistance (also known as tip or end-bearing capacity/resistance) to the total bearing capacity of piles can change significantly, not only with the interaction between soil and pile tip, but also with the mobilization of shaft (skin) friction along the piles. This can be classified into three different cases as demonstrated in Figure 1. In Case 1, the base resistance develops quickly with increasing settlement and bears most of the applied load, whereas the shaft resistance is insignificant (i.e., end-bearing piles). This case can occur when piles are short and are seated directly on a rigid stratum (e.g., shallow bedrock), while the surrounding soils are soft and contribute a minimal resistance to the axial load. For this end-bearing context, the well-known hyperbolic form is often found relevant to describe the relationship between the base resistance and settlement [6–8]. On the other hand, in Case 2, the base resistance is negligible as the soil underneath the pile tip is soft and gives insignificant resistance to the applied load (Figure 1b). This case can be observed in many coastal regions such as the Mekong Delta, Bangkok and Jakarta, where soft soil layers (SPT < 10) can reach up to 40 m [9,10]. In this context, despite using very long piles, the pile tip cannot reach a rigid layer, so there is a minimal contribution from the base to the pile bearing capacity. Finally, Case 3 occurs when both shaft and base resistances

are considerable for the entire bearing capacity. In this case, determination of how base resistance can develop with increasing load and settlement becomes much more challenging because of the complex load-transfer along the depth and the corresponding response of soil–pile interaction at the base [11,12]. For example, when the base soil is medium and fine sand, the base resistance can slowly increase due to the high compressibility of the soil underneath before reaching a larger magnitude at later stages. In fact, Case 3 is very common in practice, especially when piles, even when very long, cannot reach the rigid layer [9,13]. In this process, the development of settlement (i.e., the displacement of pile head) is the key indicator for the mobilization of the load bearing mechanism. Nevertheless, the use of settlement to assess behaviour of base resistance, especially for long piles in soft soil, has not been considered and employed effectively in design practice.

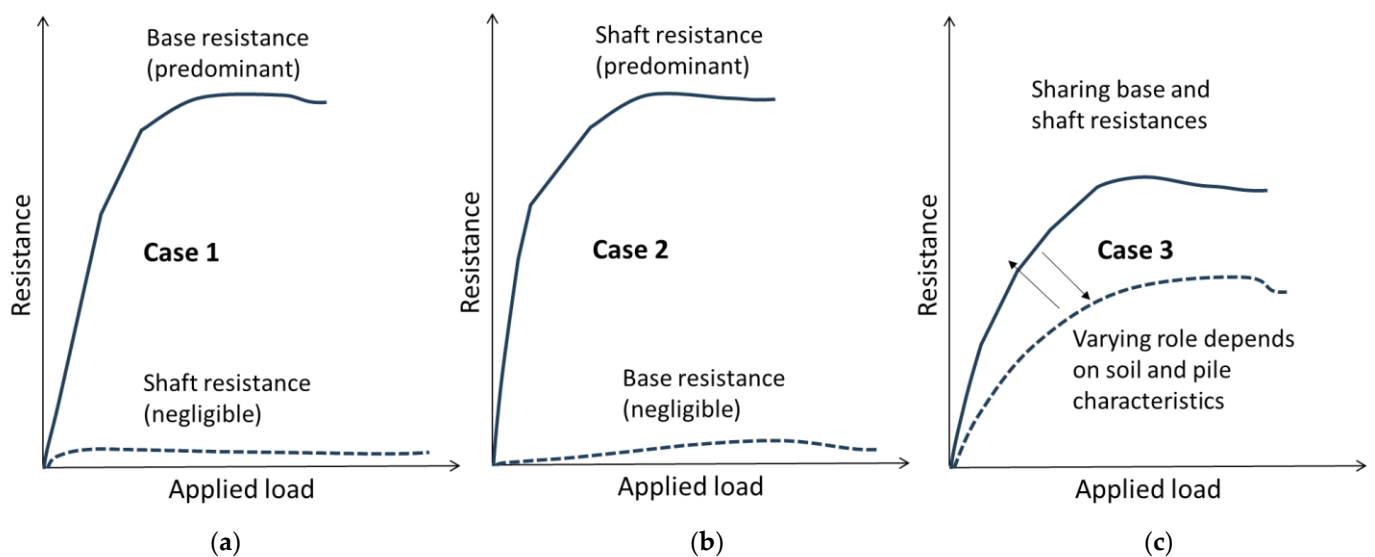


Figure 1. Contributions of base and shaft resistances to the total bearing capacity of piles in 3 different cases: (a) Case 1, where the base resistance is predominant; (b) Case 2, where the shaft resistance is predominant; and (c) Case 3, where both the base and shaft resistances are significant contributors to the total bearing capacity.

The propagation of load along a pile significantly depends on the pile geometry and its interaction with surrounding media. For very long piles, such as those commonly used in Ho Chi Minh City (50–100 m long), the base resistance only becomes significant when the pile tip presses the soil underneath to a certain degree under vertical compression load. This is because the shaft friction usually takes the majority of the applied load at the initial stage before the soil–pile interaction propagates downward with larger contribution from the base resistance [14,15]. In soft soil regions, such as the Mekong delta where the layer of soft clay ($SPT\ N \approx 0-5$) can exceed 25–35 m [10], the pile toe is normally required to sit on a hard soil layer at extremely great depths (e.g., coarse to medium dense sand layers at a depth of 70–100 m), resulting in a significant but complex contribution of base resistance to the entire bearing capacity of piles. Although this topic has received considerable attention in recent years, most previous studies could only examine short and medium piles (<45 m) [16–19], while understanding of how the base resistance of long piles can develop with increasing settlement is still limited due to the complexity and excessive cost of in situ pile tests. In fact, many empirical equations have been proposed to describe the relationship between base resistance and settlement, but they usually vary significantly with different types of soil and pile, resulting in a certain confusion in practice [11]. Predicting the base resistance and advancing our understanding of the influencing factors are thus crucial to the practical design of long pile foundations.

In recent years, machine learning (ML) has emerged as a preferable and effective approach, not only to predict various geotechnical issues, but also to assess the interaction

between different features [20–22]. Past ML applications, including the artificial neural network (ANN) and other advanced algorithms for pile foundation, have mainly focused on prediction of pile bearing capacity and settlement as highlighted in recent review studies, e.g., Baghbani et al. (2022) and Nguyen et al. (2023b) [23,24]. For example, many studies [25,26] employed shear parameters of soil from laboratory and field tests, including SPT and CPT data, to build ML models for predicting bearing capacity and settlement of piles, while the basic settlement-loading curves have also been used [20,27]. Nevertheless, there is a lack of attention to using ML to predict components of pile bearing capacity such as the skin friction and base resistance, mainly because of the complexity in measuring these individual parameters in the field. Further, the database collected for establishing ML models was relatively limited in past investigations, e.g., only short and medium piles were considered, while mobilized base resistance with increasing load was still overlooked due to the lack of appropriate field tests. Recent efforts have been made to predict base resistance of long piles based on more than 1100 datapoints collected from different real-life projects [9]; however, this study used a conventional basic ANN model, resulting in a relatively medium level of prediction quality (i.e., $R^2 = 0.8\text{--}0.87$). More importantly, the past applications of ML for pile foundation were often criticized for their black-box nature regarding, e.g., the unseen interactions among different features and the lack of validation with existing methods. In fact, an insightful interpretation of the key role of settlement on pile bearing capacity, including the base resistance that can employ an effectively advanced ML and post-analysis techniques, is still missing. Therefore, more attempts, not only to develop robust ML models for predicting pile's base resistance, but also to advance our understanding of settlement-base resistance interaction become necessary.

In view of the above, this paper aims to advance our understanding of how the base resistance of long piles (approximately 57–90 m) can behave when the pile settlement increases. A novel method combining extensive field data and advanced analysis based on machine learning techniques is adopted. Data from various field tests (86 piles in 37 different projects) on bored piles installed in the very soft soils of the Mekong Delta are used to form empirical relationships between the base resistance and settlement of piles, followed by development of advanced ML models adopting XGBoost and Random Forest (RF) algorithms. This approach enables different soils and piles to be incorporated into a universal model through a training process, eliminating the confusion in using empirical equations, which often change widely with different factors. It is worth noting that, while adopting the existing ML algorithms, major innovations are the new understanding of base resistance behaviour when piles are very long and installed in soft to medium soils with reference to common practical methods. The novel outcomes are not only the cost-effective prediction of pile base resistance, but also the assessment of the role of pile settlement on base resistance behaviour, giving significant value to the practical design of pile foundation.

2. Influence of Settlement on Base Resistance through Field Investigations

2.1. Overall Review of Field Investigation and Pile Features

An extensive site investigation over the past 10 years of pile foundation practice in the Mekong Delta (South of Vietnam) was carried out to improve understanding of the base resistance of piles in soft soil [9]. The investigation went through 37 different high-rise building projects located on the very soft ground of Ho Chi Minh City, Vietnam (Figure 2a), resulting in a collection of 86 different long and large piles. These piles were selected for detailed assessment because they were all longer than 40 m (classified as long to very long piles) and subjected to static load tests where instrumentation enabled the shaft and base resistances to be estimated. They had an equivalent diameter ranging from 1.0 to 2.5 m and a length of up to nearly 100 m, and were installed on complex geological strata, including various soft soil layers. Figure 2b shows a typical profile of the ground near the Mekong River. The soft to very soft soil layer ($SPT < 5$), which would make a minor contribution to the pile bearing capacity, can reach up to 35 m in depth. On the other hand, Layer 4, i.e., 30–40 m thickness of dense fine to coarse sand, can be the largest contributor to the shaft

(skin) resistance of piles. The SPT of soil only exceeded 50 at a depth > 70 m (dense sand), which is also the normal required depth for pile embedment, thus very large and long piles are often used for high-rise buildings in this region.

Apart from the conventional static load test (SLT), which is often relevant to bored piles in a sufficiently large space with test load less than 4500 tons, the O-cell load test (OLT) was adopted for super-long piles (usually > 60 m) in limited space conditions with test load greater than 4500 tons. The major advantage of these pile tests compared to many others in previous studies was the installation of strain gauges along the pile and near the toe (i.e., 0.5–1 m above the pile tip) to estimate the load distribution during testing, enabling the shaft and base resistances to be estimated. Compared to previous studies where machine learning techniques were applied to pile foundations [20,23,27,28], the piles investigated in this study were certainly longer, larger and embedded through various soft soil strata, thereby exhibiting a more complex and distinct behaviour.

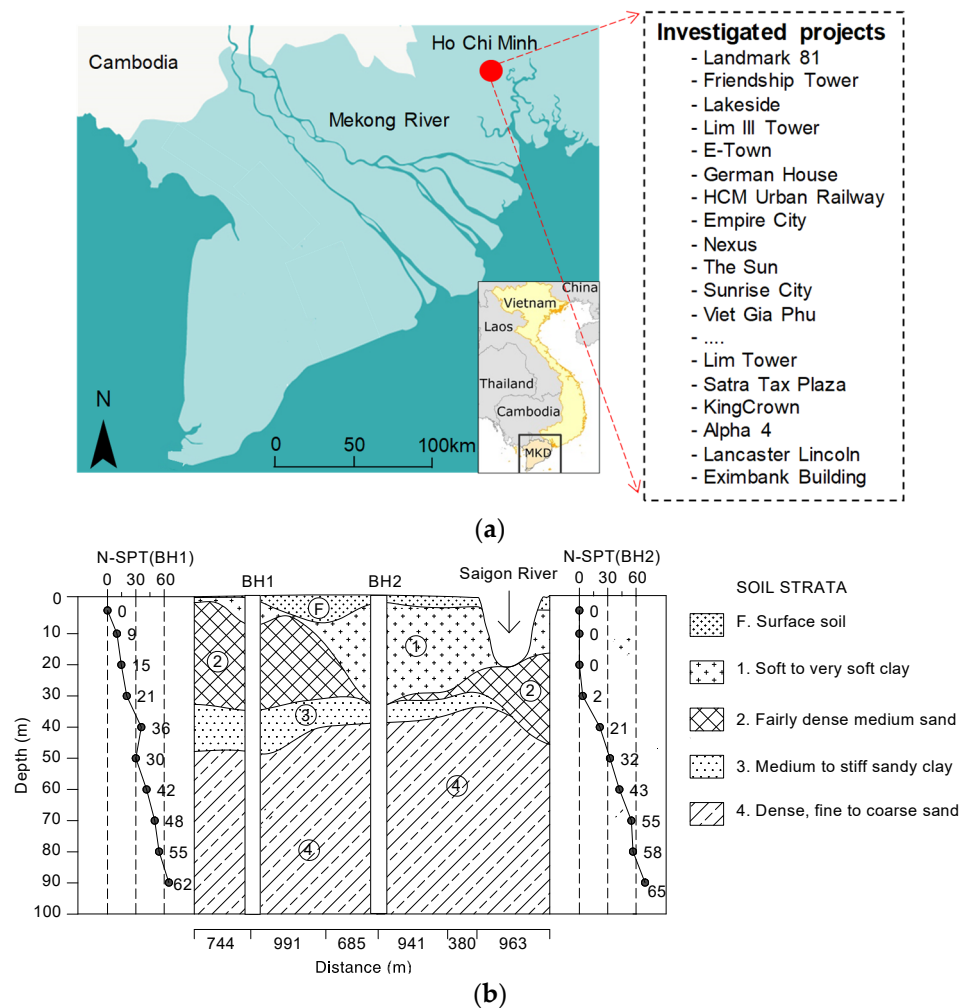


Figure 2. (a) Location of the investigated projects relative to the Mekong River delta, and (b) typical geological profiles near the Mekong River.

With reference to the previous findings [9], 5 key parameters, including the applied load (P_t), settlement (S or the displacement of loading point), axial stiffness (i.e., $A \times E$, where A is the cross-sectional area of pile, and E is the equivalent Young’s modulus, $E = 36$ GPa), SPT values (N) of the soil beneath the pile toe, and the distance from the loading point to the pile toe (L_e), were considered in the current analysis. Figure 3 and Table 1 summarize key information of the pile tests used in this study. It is noted that the distance from the loading point to the pile toe was the same as the embedded length (Figure 3a) for

SLT, but this was not the case for OLT as the loading point was not identical to the pile head in this type of test. The results show that the ultimate test load varied from approximately 1000 to around 6000 tons, whereas the maximum displacement of loading point (settlement) exceeded 230 mm. In fact, many of the tested piles had maximum displacement of less than 50 mm, indicating that the pile tests seemed not to have been carried out up to ultimate failure. The equivalent diameter of piles changed from approximately 1 to 2.5 m (Figure 3b) and the SPT value of soil beneath the pile toe was in the range between 26 and 70 (Figure 3c). Through these pile load tests, a database of 1131 load-displacement points was collated in tandem with the measured unit base resistance Q_b for building appropriate ML models. It is also noteworthy that this database only encompasses long to very long piles ($L > 40$ m) where the base resistance measured during loading is available.

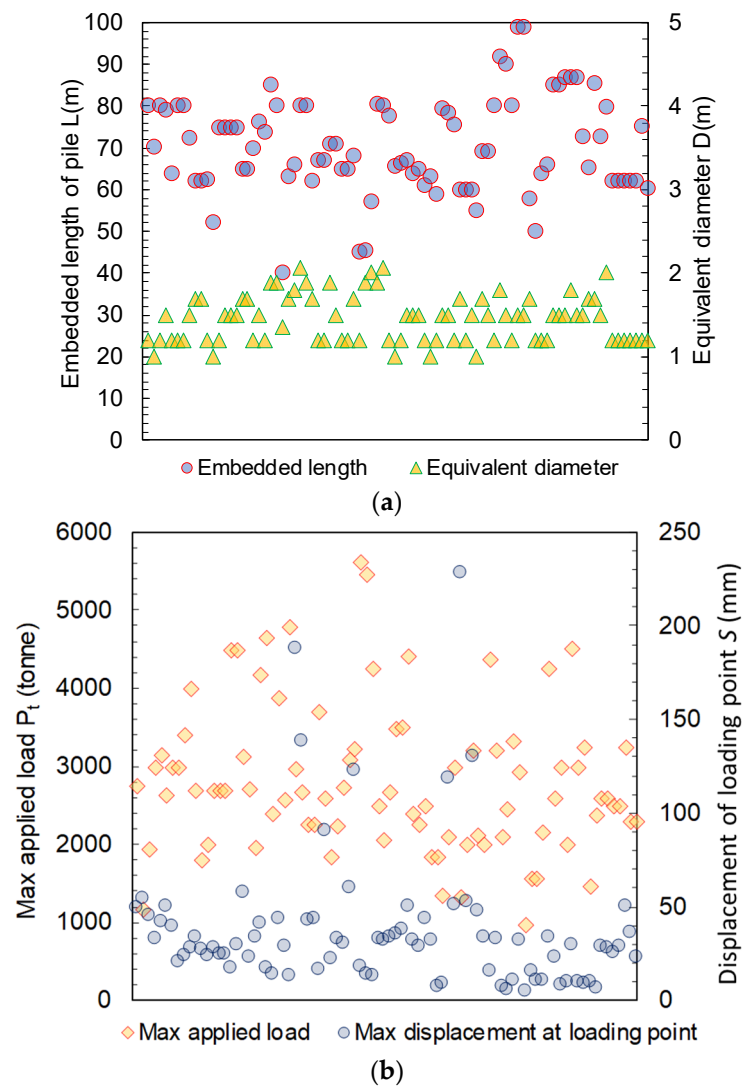


Figure 3. Cont.

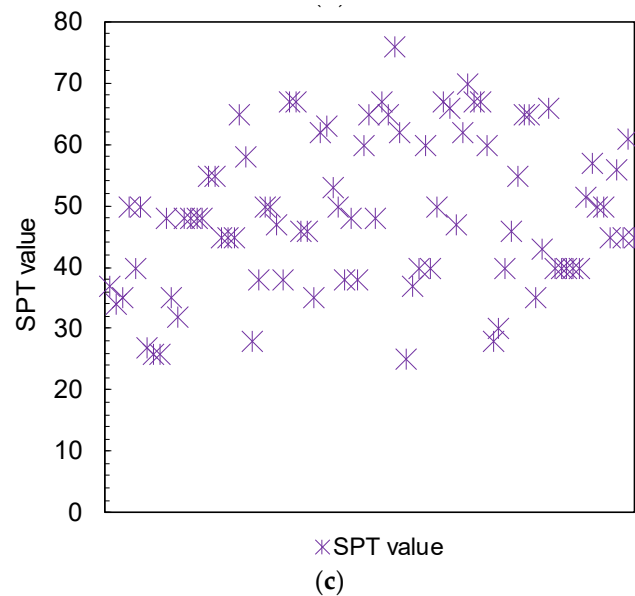


Figure 3. Distribution of the tested pile’s primary features: (a) the embedded length and equivalent diameter, (b) the maximum applied load and settlement, (c) the SPT value of soil beneath the pile toe.

Table 1. Key information for pile load tests (full data can be downloaded from the link: <https://zenodo.org/records/11029735>).

| Features | Applied Load P_t (Tonne) | Settlement of Loading Point S (mm) | Distance from Loading Point to Pile Toe L_e (m) | SPT of Soil Beneath Pile Toe (m) | Equivalent Diameter D (m) | Embedded Pile Length L (mm) |
|----------|----------------------------|--------------------------------------|---|----------------------------------|-----------------------------|-------------------------------|
| Min | 162.5 | 0.10 | 8.00 | 23.00 | 1.00 | 40.20 |
| Max | 5625.0 | 228.00 | 80.30 | 76.00 | 2.07 | 99.00 |
| Mean | 1749.8 | 12.80 | 44.52 | 50.11 | 1.49 | 72.45 |

2.2. Behaviour of Base Resistance in Short and Medium Piles

Previous studies [16,29–32] have proved the considerable impacts that settlement can have on the developed base resistance of pile foundation. However, these studies were restricted to short and medium piles, while quantitative data for long piles (>60 m) are still limited, as shown in Table 2. In fact, the pile length investigated in past studies was normally less than 35 m, which is much shorter than those considered in the current investigation. Figure 4 shows how the contribution of the base resistance, i.e., P_b/P_t , changes with different degrees of settlement in short piles. It is worth mentioning that, in this consideration, P_b is the total reaction force, whereas Q_b is the pressure under the pile toe, i.e., the base unit load [7]. Both P_b and Q_b can represent the base resistance (i.e., $Q_b = P_b/A$); however, P_b is used herein to compare with the total applied load P_t for the unity. Figure 4a undoubtedly indicates that the base resistance–settlement relationship of short and medium piles complies with the well-known hyperbolic form, i.e., [6]

$$\frac{P_b}{P_t} = \frac{S}{a + bS} \quad (1)$$

where a and b are the constants changing with different soils. In this description, P_b rapidly develops at the initial stage and then becomes stable, despite the increasing settlement. Nonlinear behaviour begins to occur when the settlement S exceeds 5–10 mm. The lower and upper bounds for these data are defined with the values of a that change from 0.033 to 0.395, while b varies slightly from 0.017 to 0.022, respectively. On the other hand, Figure 4b

shows the combination of data from the previous and the current site investigations. It is important to note that the current data for short piles were obtained from O-Cell tests where the loading points were placed 20 to 30 m away from the pile toe. The length from the loading point to the pile toe is termed as “effective length” (L_e), which is different from the real (physical) length of the piles (57–90 m). For this extension of data, the value of a becomes wider, i.e., $a = 0.055$ to 0.93 . This indicated that the distance from the loading point to the base, i.e., the effective length, plays a crucial role in the load transfer behaviour of piles.

Table 2. Summary of long piles loaded up to ultimate failure in this study and short/medium piles from previous studies.

| Project Name/References | Test Pile Name | D (m) | L (m) | L_e (m) | P_t (Max) (Tonne) | S (Max) (mm) | P_b/P_t (Max) (%) | SPT of Soil Beneath Pile Toe |
|--|----------------|---------|---------|-----------|---------------------|----------------|---------------------|------------------------------|
| Long piles $L = 60$ – 80 m, Static load tests (SLT) in the current study | | | | | | | | |
| Viet Gia Phu | TP02 | 1.2 | 80.0 | 80.0 | 2640 | 59.2 | 36.6 | 50 |
| Lakeside | TP2 | 1.2 | 80.0 | 80.0 | 2750 | 49.5 | 15.8 | 37 |
| Acent Plaza | PTB | 1.0 | 70.3 | 70.3 | 1170 | 54.7 | 24.5 | 35 |
| | PTA | 1.2 | 80.3 | 80.3 | 1950 | 45.4 | 20.6 | 38 |
| Friendship Tower | TP2 | 1.2 | 64.0 | 64.0 | 3150 | 42.6 | 14.6 | 50 |
| Vietcombank Tower | TBP2 | 1.5 | 70.8 | 70.8 | 2604 | 90.7 | 33.0 | 46 |
| Green Towers | TP1 | 1.5 | 63.8 | 63.8 | 3500 | 37.9 | 22.6 | 60 |
| Vinhomes Bason | TN2 | 1.2 | 60.0 | 60.0 | 3000 | 51.5 | 18.2 | 45 |
| Empire City | TSBP7-MU7 | 1.2 | 62.2 | 62.2 | 3250 | 50.3 | 12.4 | 40 |
| Short and medium piles $L/L_e < 35$ m, O-cell load test (OLT) in the current study (L_e is considered) | | | | | | | | |
| Vinhomes Golden River | TN1 | 1.7 | 60.0 | 12.0 | 2100 | 120 | 43.2 | 45 |
| Landmark Tower | TN3 | 1.5 | 60.0 | 8.0 | 1325 | 225 | 72.0 | 50 |
| Hilton | TP2 | 1.9 | 80.0 | 22.2 | 4659 | 17.3 | 15.0 | 58 |
| Lancaster Nguyen Trai | TP2 | 1.9 | 80.0 | 22.0 | 2531 | 30.0 | 13.3 | 47 |
| Viettinbank | TP1 | 1.7 | 62.0 | 15.0 | 2758 | 40.0 | 23.6 | 38 |
| KingCrown | TP5 | 2.0 | 57.0 | 10.3 | 5625 | 17.9 | 25.6 | 62 |
| Bason | TP1-1 | 1.5 | 78.5 | 21.0 | 1850 | 32.4 | 23.4 | 76 |
| | TN1 | 1.7 | 60.0 | 12.0 | 2105 | 119 | 43.5 | 50 |
| | TN3 | 1.9 | 60.0 | 8.0 | 1850 | 210 | 69.0 | 55 |
| The Sun | TN6 | 1.7 | 69.0 | 10.5 | 3206 | 130 | 43.7 | 52 |
| | TP2 | 1.5 | 90.0 | 19.0 | 3202 | 32.8 | 20.8 | 62 |
| Static load test (SLT) in the previous studies | | | | | | | | |
| [30] (Al-Atroush et al., 2020) | LDBP | 1.3 | 9.5 | 9.5 | 325 | 70.0 | 37.6 | NA |
| [33] (Eid et al., 2018) | - | 1.0 | 34.0 | 34.0 | 900 | 23.5 | 16.7 | 83 |
| [29] (Liu et al., 2020) | TP1 | 0.8 | 25.8 | 25.8 | 723 | 46.0 | 54.3 | NA |
| | TP2 | 0.8 | 25.5 | 25.5 | 779 | 42.0 | 44.3 | NA |
| | TP3 | 0.8 | 25.6 | 25.6 | 779 | 47.0 | 38.5 | NA |
| [16] (Bai et al., 2020) | TP1 | 0.5 | 25.5 | 25.5 | 900 | 44.0 | 33.3 | NA |
| | TP2 | 0.5 | 26.5 | 26.5 | 900 | 47.0 | 42.2 | NA |

Note: D is the diameter (or equivalent) of pile; L is the physical length of pile; L_e is the effective length of pile (i.e., distance from the loading point to pile toe); P_t is the applied load, S is the settlement (displacement) of the loading point, P_b is the base resistance force.

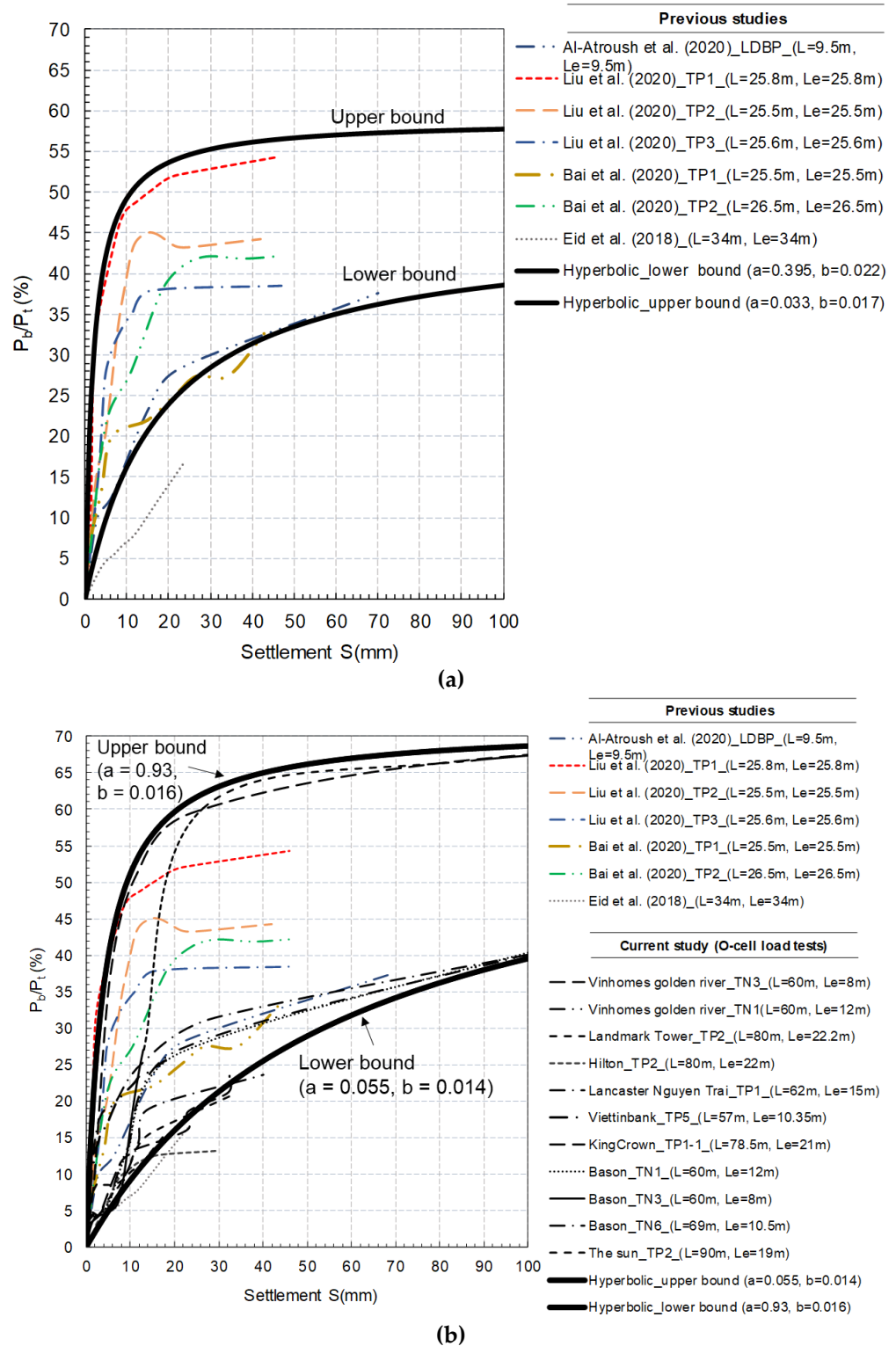


Figure 4. Contribution of base resistance to the total bearing capacity of short and medium piles in comparison with hyperbolic model: (a) previous studies [16,29,30,33]; and (b) combined previous studies and the O-cell test data in the current study.

2.3. Response of Base Resistance in Long Piles

For very long piles where the length can exceed 60 m and even reach 100 m as addressed in the current study, the measured data (Figure 5) show significant difference in the response of base resistance compared to short and medium piles. It is important to note

that only very long piles ($L > 60$ m) subjected to the static pile load test, where the length of piles was identical to the distance between the loading point and pile toe, are considered in this analysis. Specifically, all the datapoints are positioned outside the short-to-medium pile region, which was defined earlier (Figure 4). The contribution from the base resistance to the total bearing capacity becomes considerably less when piles are longer than 60 m for the same magnitude of settlement. Furthermore, unlike short and medium piles, it is apparent that the P_b - S curves of long piles do not comply with the conventional hyperbolic form, as the P_b develops much more slowly at an early stage. In fact, there are two distinct stages in the development of base resistance P_b with respect to increasing settlement S that can be detailed as follows.

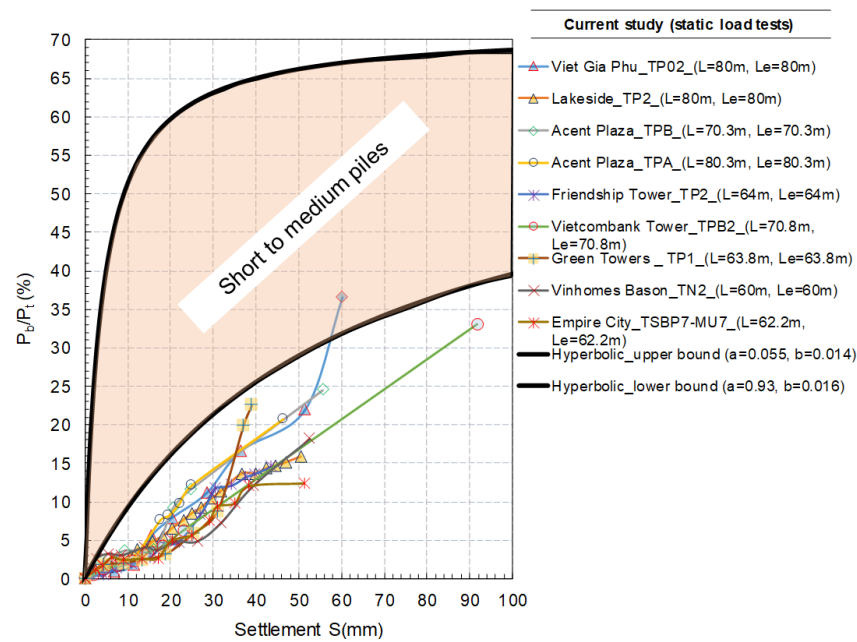


Figure 5. Base resistance of long piles in comparison with short and medium piles.

Stage 1 ($S < 20$ mm): In this early stage, when the pile head settlement is less than 20 mm (Stage 1), most of the bearing capacity is derived from the shaft resistance that develops with pile–soil interactions (friction and cohesion), while the base resistance accounts for less than 5% the total applied load.

Stage 2 ($S > 20$ mm): When the settlement further increases, the curve apparently changes its slope. Specifically, the slope gradient doubles, indicating larger contribution from the base resistance to the total bearing capacity when S becomes larger than 20 mm. As S increases to 40 mm, the contribution ratio P_b/P_t extends by a factor of nearly 3, (i.e., P_b accounts for approximately 15% P_t) compared to when $S = 20$ mm. As the settlement of pile head continues to increase, the contribution of the base resistance to the total bearing capacity continues to increase, eventually exceeding 20% when the settlement is greater than 50 mm. In comparison with short and medium piles, this contribution is certainly much smaller. The nonlinear relationship of the contribution ratio P_b/P_t and settlement (i.e., the dark blue trend line in Figure 6) can be described by Equation (2) with a relatively high degree of correlation coefficient ($R^2 = 0.89$). Despite its simplicity, this empirical equation can have a significant implication for the practical design of pile foundations, as one can estimate the contribution ratio P_b/P_t for a long pile if the settlement is known.

$$\frac{P_b}{P_t} = -0.00006S^3 + 0.0087S^2 + 0.1166S + 0.5 \tag{2}$$

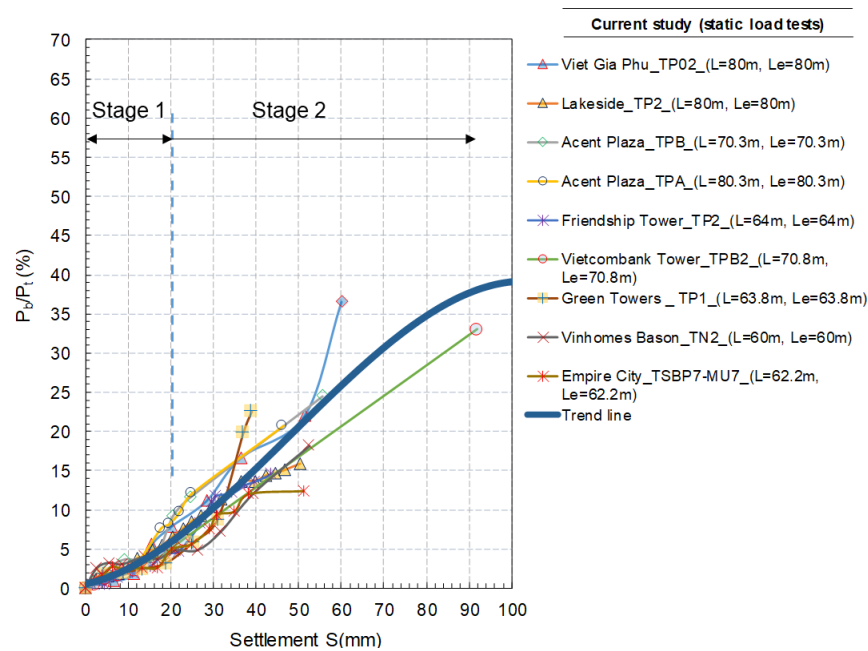


Figure 6. Two different stages in the development of base resistance over increasing settlement in long piles ($L_e \geq 60$ m).

It is important to note that the above equation should be applicable for $S \leq 90$ mm due to the lack of data in a greater range. Furthermore, more data are required to improve the prediction confidence when S varies from 60 to 90 mm.

2.4. Modified Hyperbolic Form for Long Piles in Soft Soil

The above results indicate that the development of P_b in Stage 1 is almost linear to increasing settlement, where the contribution of base resistance is relatively low. This happened because: (i) the shaft resistance (skin friction) is predominant in the early stage for long piles, making the contribution from base resistance insignificant (<5% of the total applied load) when $S < 20$ mm; (ii) the settlement of the pile head propagated downward and this occurred over a long distance through soil–pile interaction in long piles, resulting in a smaller displacement of pile toe compared to that in shorter piles. In fact, the measurement of displacement at the pile toe indicated that this displacement was about 15–20 mm less than the settlement of the pile head. When $S > 20$ mm, it triggered significant mobilization of shaft resistance (slippage between pile and soil associated with decreasing friction), and thus a substantial growth in the contribution of base resistance to the total bearing capacity. Considering the critical threshold $S_c = 20$ mm, a modified hyperbolic form for long piles to predict the base resistance can be proposed as follows:

$$\frac{P_b}{P_t} = 0.25S \tag{3}$$

$$\frac{P_b}{P_t} = \frac{S - 20}{1.5 + 0.0135(S - 20)} + 5 \tag{4}$$

By replacing $(S - 20)$ by S' to account for the initial delay before the greater contribution from the base resistance, Equation (4) becomes the ordinary hyperbolic form, as shown in Equation (1), i.e.,

$$\frac{P_b}{P_t} = \frac{S'}{1.5 + 0.0135S'} + 5 \tag{5}$$

3. Machine Learning Approach to Assess the Role of Settlement on Base Resistance

3.1. Selection and Algorithms for Machine Learning Models

There are various Machine Learning (ML) algorithms that have been developed and successfully applied to pile foundation in recent years, among which XGBoost and Random Forest (RF) have shown the best performance [21,25]. Therefore, these two algorithms were selected to predict base resistance, as well as in assessing the role of pile settlement. The field data described earlier (Figure 3) were employed for the training model with five input variables, i.e., P_t , S , AE , SPT_N and L_p . Both XGBoost and RF belong to the ensemble learning family; however, while RF uses the bagging algorithm, XGBoost is an effective representative for the boosting concept. It is worth mentioning that the ensemble learning method can have two different approaches, i.e., (i) bagging (also known as bootstrap aggregating), where the learning is made in parallel through independent decision trees and subsets, whereas in boosting technique (ii), the learning occurs sequentially and adaptively to improve prediction through each decision tree. The differences in these two algorithms and their implementations in the current database are represented in Figure 7. Further details of these techniques, including their mathematical formula, have been given in various past studies [21,34], so they are not further repeated in this paper for brevity.

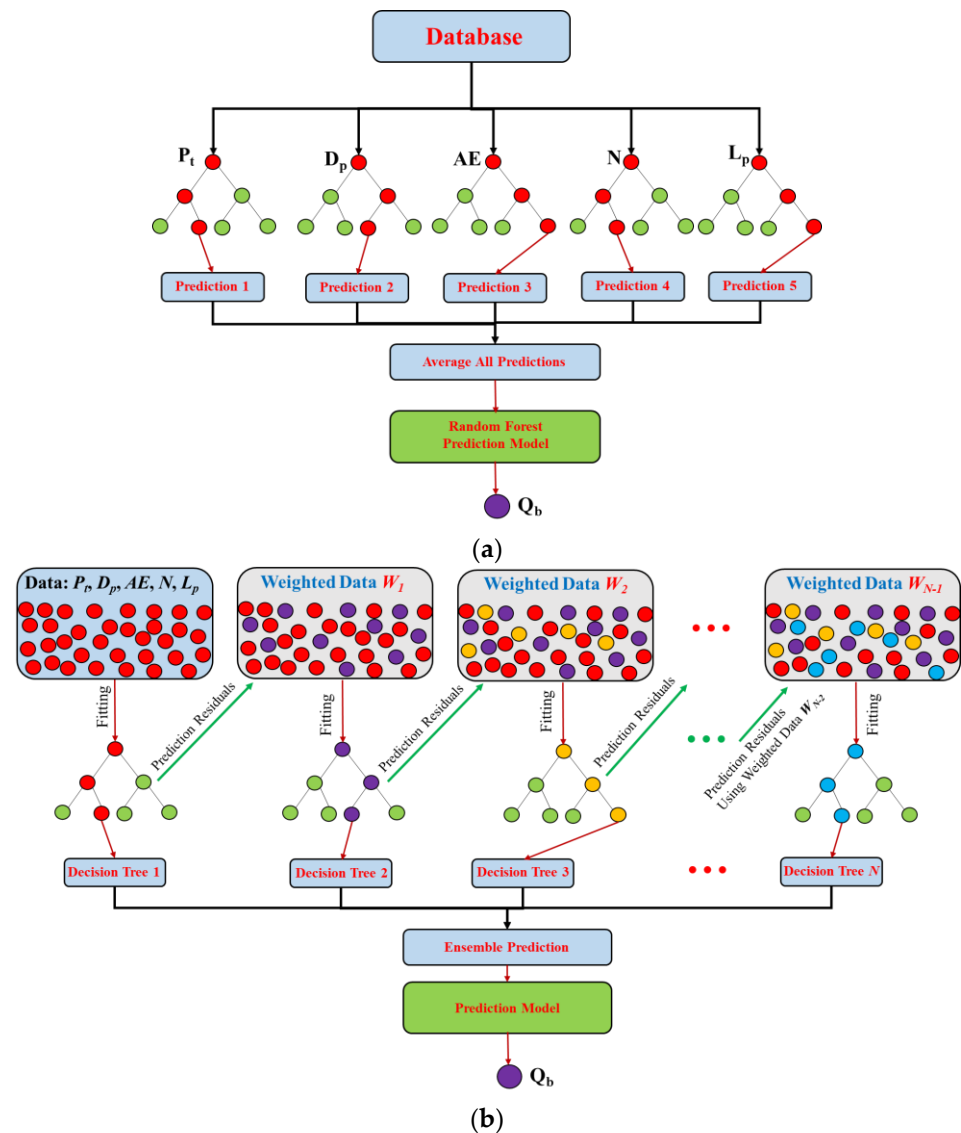


Figure 7. Model implementation using the collected database: (a) Random Forest; and (b) XGBoost.

In the current study, apart from the conventional majority voting that is commonly implemented to understand feature importance in ML modeling, the SHAP (SHapley Additive exPlanations) analysis technique was also used for detailed characterization [35]. The Shapley value (also known as SHAP value) was computed as the averaged sum of marginal contributions from individual features j as follows:

$$\phi_j(x) = \frac{1}{M} \sum_{m=1}^M \phi_j^m \quad (6)$$

where M and j are the number of iterations and the feature index, respectively. The marginal contribution $\phi_j^m = \hat{f}(x_{+j}) - \hat{f}(x_{-j})$ with \hat{f} is the prediction model. Compared to other evaluation methods, SHAP is developed based on a more solid theory that overcomes the limitations of earlier methods, such as LIME, thus ensuring fair contributions among different features [36,37]. Further, SHAP, via the Shapley value, allows a contrastive explanation to be obtained, promoting understanding of both sides (negative and positive impacts) that a feature can cause for the targeted prediction.

3.2. Data Processing, Model Training and Validation

For model training, 85% of the original dataset was randomly selected, and the remaining 15% was used for testing the established model. For equal treatment of datapoints during this division, the stratified sampling method, where the entire database was first divided into different groups (or strata) based on their shared characteristics, was applied. This division was applied consistently for both XGBoost and Random Forest algorithms. To enhance the training performance, the K -fold cross validation method was adopted to ensure model stability and predictive performance. In this process, the training dataset was sub-divided into 10 folds in which 9 folds were used for training and the rest for cross-validation. This process was repeated through each fold so that the validation was made 10 times across different subsets, thus giving an equal treatment for datapoints. The trained model through a 10-fold cross-validation process was then used to predict the remaining 15% of the dataset for testing purposes. The outcomes from cross-validation were assessed, in addition to the prediction of testing data, further reinforcing the rigor of the assessment method. To assess the model performance, the coefficient of determination (R^2) and root mean squared error (RMSE) were calculated.

Figure 8 shows the performance of XGBoost and RF models through 10-fold cross-validation during the training phase. The results indicate the more reliable and accurate prediction given by XGBoost. For example, the mean R^2 for XGBoost is nearly 90%, whereas it is about 86% for the RF model. Further, the RMSE induced by XGBoost is about 320, which is relatively lower than that made by RF. Figure 9 compares the measured and predicted data using the two built models based on the XGBoost (Figure 9a) and Random Forest (Figure 9b) algorithms. The results show highly accurate predictions by the two models, i.e., RF and XGBoost, when their R^2 values are nearly 90% and 92.7%, respectively. The XGBoost algorithm yielded better performance, as it produced a larger R^2 compared than its counterpart. In fact, XGBoost had almost perfect success in training, with R^2 approaching 100%, followed by a high degree of R^2 in the testing phase, indicating that no over-fitting that had occurred. The assessment proved the success in building machine learning models for predicting the base resistance of pile foundations, and thus the confident use of model outcomes for advancing our understanding of the influencing factors on base resistance. It is also important to note that using different subsets of data for training and validation resulted in variation in model performance (varying R^2 and RMSE). This was because of the non-uniformity of data, causing varying features of data subsets, which can be minimized by using a larger and more complete database [24,38].

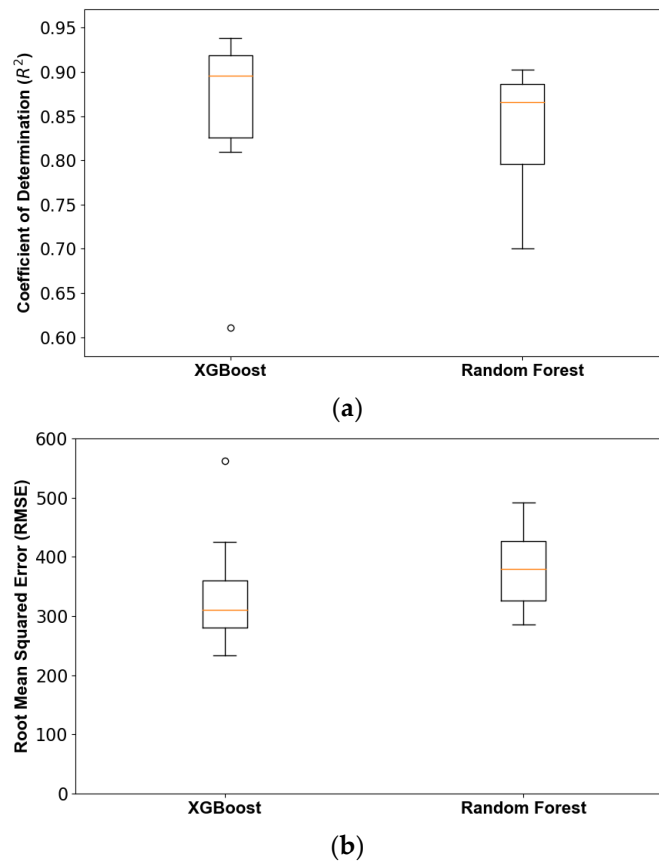


Figure 8. Performance of XGBoost and Random Forest (RF) models through 10-fold cross validation using 85% of the original dataset: (a) coefficient of determination; and (b) root-mean-squared error.

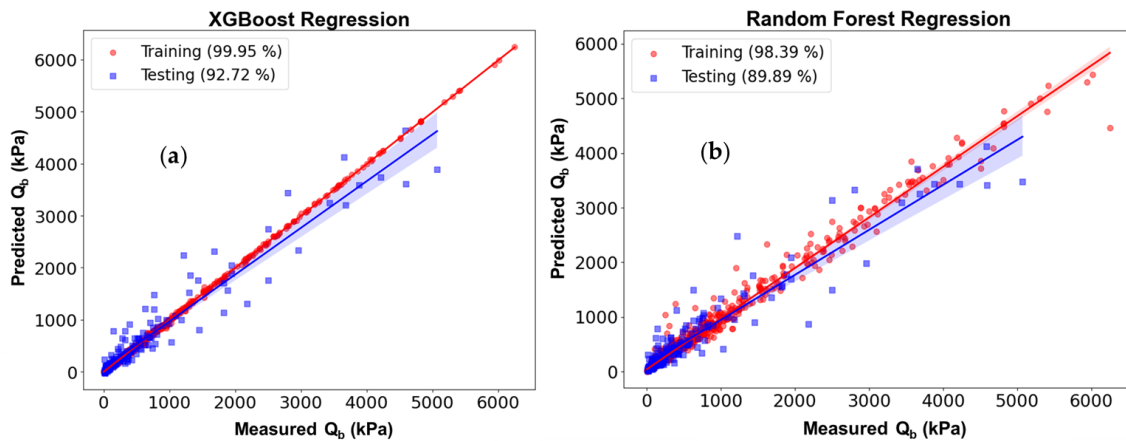


Figure 9. Coefficient of determination (R^2) of model predictions by: (a) XGBoost; and (b) Random Forest.

3.3. Assessment of the Role of Settlement through Machine Learning Outcomes

In this section, the earlier established machine learning models are used to advance our understanding of the influence that settlement can have on the behaviour of base resistance Q_b of the pile foundation. Figure 10 presents the results from SHAP analysis for the impacts that different input features have on Q_b . The results confirm the most impactful role of settlement on the base resistance, as this feature received the largest mean score, i.e., approximately 350, which is agreed by both XGBoost and RF models. This score is significantly larger than those induced by the second and third impactful features, i.e., the applied load P_t and axial stiffness AE. Interestingly, the stiffness of soil beneath the pile toe

(SPT value), which is often believed to be one of the most important factors influencing the base resistance [7,39], received the lowest score (around 100 and 75 by XGBoost and RF, respectively). This was because all the collected long piles in this investigation sat on relatively the same soil condition, i.e., the N value mostly varied in a narrow range from 40 to 70 (dense to very dense sandy soil), as shown in Figure 3. The positive and negative scores from the SHAP analysis (Figure 10b,d) represent how the features influence the predicted outcome. The predominant range of high positive scores (red at the right-hand side) by settlement indicates that this factor has mainly a positive impact, i.e., a progressive relationship, on the base resistance. On the other hand, the scores for axial stiffness are distributed at both negative and positive sides of the charts, meaning that increasing axial stiffness does not always lead to larger base resistance of piles.

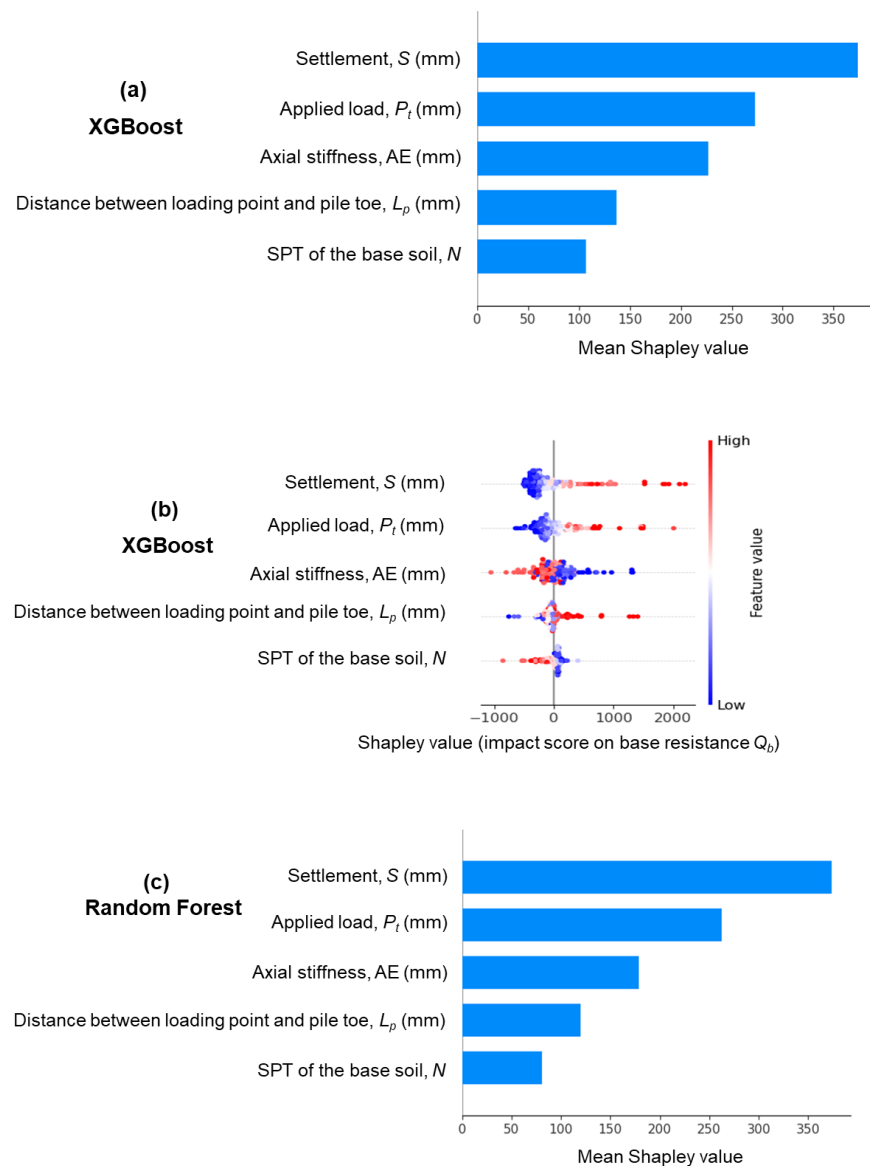


Figure 10. Cont.

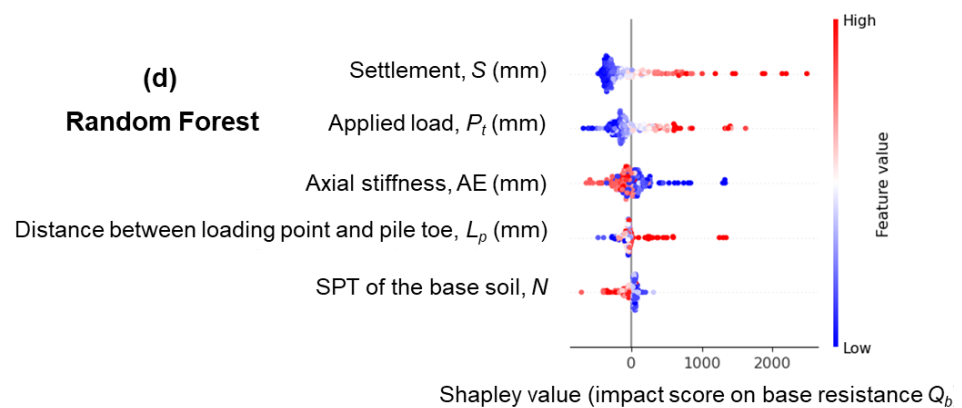


Figure 10. Assessment of influencing factors on base resistance Q_b using SHAP method: (a,b) XGBoost; (c,d) Random Forest (RF).

The relationship between the settlement and base resistance can be quantified using the partial dependence plot based on the trained machine learning models, as shown in Figure 11. In this analysis, the settlement was varied in a given range, e.g., 0 to 50 mm, and combined with other inputs to form various datasets based on Monte-Carlo theory. The average predicted Q_b corresponding to each value of settlement S can then be used to create the partial dependence plot, i.e., [36]

$$f_S(x_S) = \frac{1}{n} \sum_{i=1}^n f(x_S, x_C^i) \tag{7}$$

where f_S is the partial dependence function for each value of settlement S (i.e., x_S); x_C represents other (input) features which are not considered in the partial dependence analysis; and n is the number of instances. The results (Figure 11) show that, when the settlement S increases from zero to around 18 mm, the base resistance Q_b slightly increases to around 1000 kPa. However, when S exceeds 20 mm, the slope of the S – Q_b curve becomes larger, indicating a stronger influence of settlement on Q_b , i.e., a bigger increase of Q_b for the same rise in settlement. Both XGBoost and Random Forest models agree very well regarding this behaviour, which in fact corroborates perfectly the observation in the field data shown earlier (Figure 6).

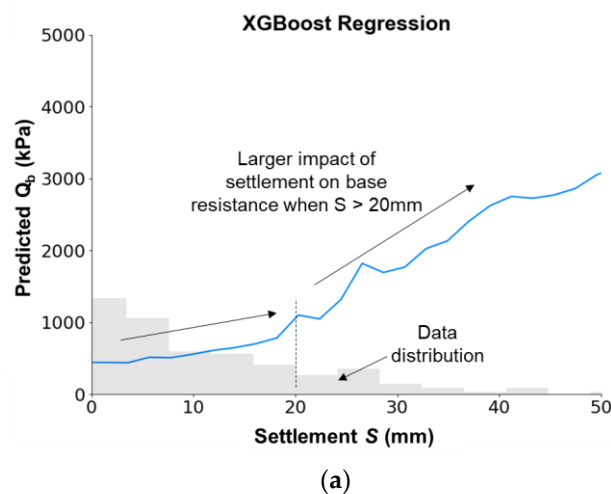


Figure 11. Cont.

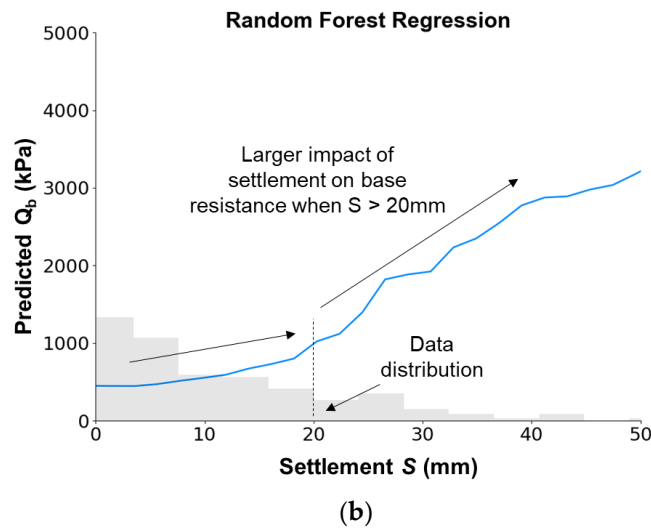


Figure 11. Influence of settlement on base resistance predicted through machine learning assessment (partial dependence plot PDP): (a) XGBoost; and (b) Random Forest.

Although the earlier partial dependence plots induced by machine learning have successfully captured the relationship between Q_b and settlement S , they can only show the average effect of S on Q_b (i.e., global method), while the variation over different instances cannot be seen. Equation (7) averages the function f_s for different instances of x_S and x_C , therefore, the individual conditional expectation (ICE) plots, which can present the Q_b – S relationship more comprehensively across various instances, are useful to understand the full range and any other different behaviour of the Q_b – S curves. Figure 12 shows this range, with the S varying up to 50 mm for the trained XGBoost and Random Forest regressions. While the centred (Red) curves are identical to the partial dependence plots, the results show considerable variation for individual instances. Most of the curves agree very well with the centred behaviour, where Q_b increases slowly at the initial stage ($S < 20$ mm) and develops more quickly for the larger settlement. There are some instances in which Q_b exhibits an opposite response, i.e., it develops rapidly at an early stage and stabilizes when S rises to 50 mm, which was probably induced by some outliers in the database.

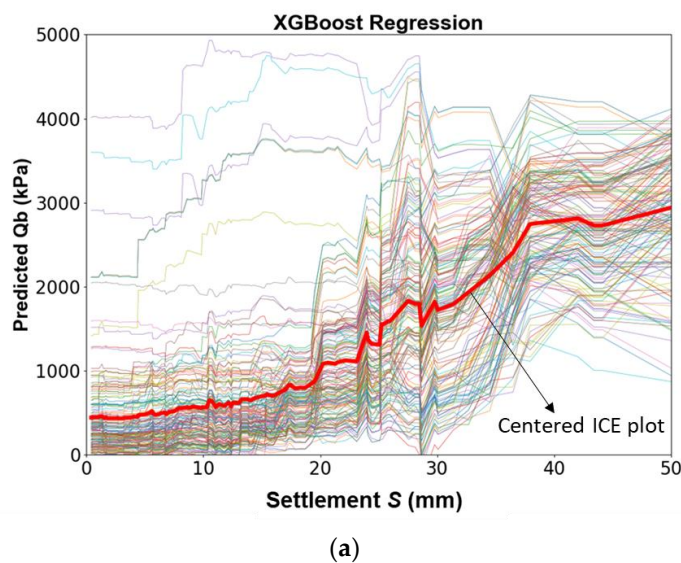


Figure 12. Cont.

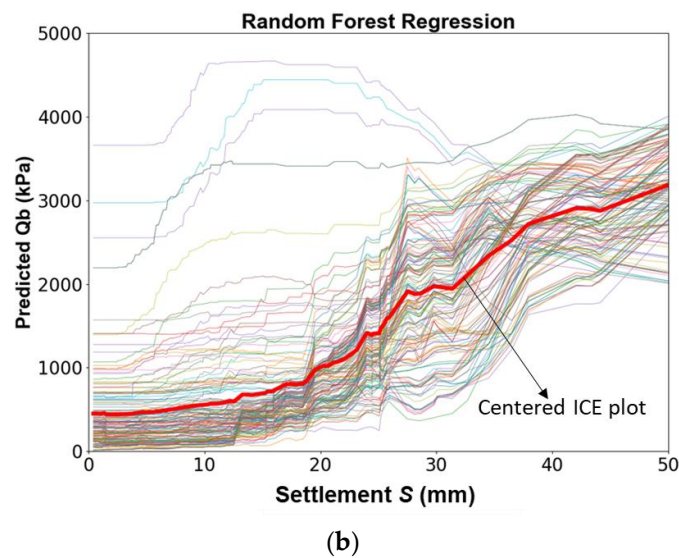


Figure 12. Individual effect of settlement on base resistance Q_b through machine learning assessment (individual conditional expectation (ICE) plots): (a) XGBoost; and (b) Random Forest.

4. Discussion and Practical Implications

The conventional hyperbolic relationship between the base resistance and settlement often considers the displacement of pile tip, which is more difficult to measure compared to that of pile head in practice. For example, during service of the pile foundation, the settlement at pile head (i.e., normally identical to the ground or basement levels) can be conveniently monitored over time, whereas the measurement of pile tip is usually challenging and costly. The current study has addressed this issue by investigating the relationship between the base resistance Q_b and the settlement of the pile head (S). The results show the considerable influence of pile length on the Q_b – S curves, i.e., the longer the piles, the slower response and the less contribution of Q_b to the increasing S . Figure 13 shows the contribution ratio of base resistance that has been normalised with the pile's length and presented over the settlement of the pile head. The results clearly show that, without the influence of pile length, the difference in base resistance behaviour among different piles is still considerable. This means that the influence of pile length is not only because of the vertical deformation (shrinkage) of pile under compression, but also due to the frictional contact between soil and pile affecting the load being transferred to the pile toe. For short piles ($L_e < 30$ m), the base resistance can account for a maximum of approximately 55% of the total bearing capacity, but it can reach only to around 30% in long piles ($L_e > 60$ m). Given the same percentage of settlement, e.g., 0.05%, the base resistance of short piles has already developed rapidly to around 80% of its maximum level; however, it increases very slowly in long piles. This suggests that, for long piles, the skin friction can account for the majority (80–90%) of the ultimate bearing capacity of piles, despite being installed in soft soil, thus appropriate consideration of this part is critical.

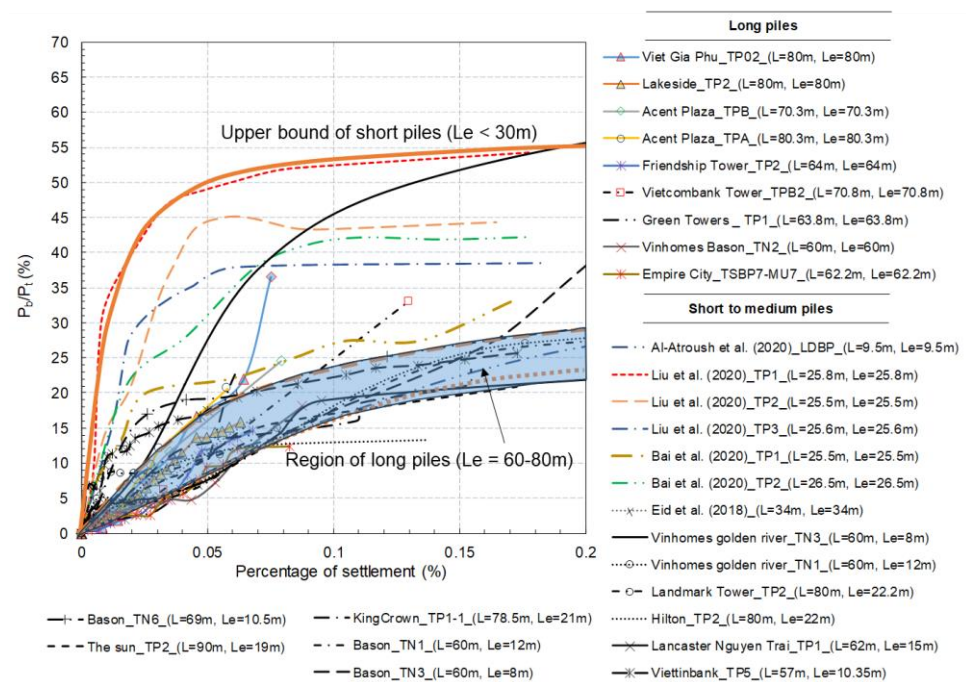


Figure 13. Contribution of the base resistance to total bearing capacity with settlement normalised over the pile length [16,29,30,33].

Figure 14 represents how well the predicted trend line by the XGBoost model matches the actual behaviour of base resistance in long piles. The data not only show the distinctive response of long piles to increasing settlement in comparison with short piles, as explained earlier, but also proves the excellent capability of the trained model, with its main focus on long piles.

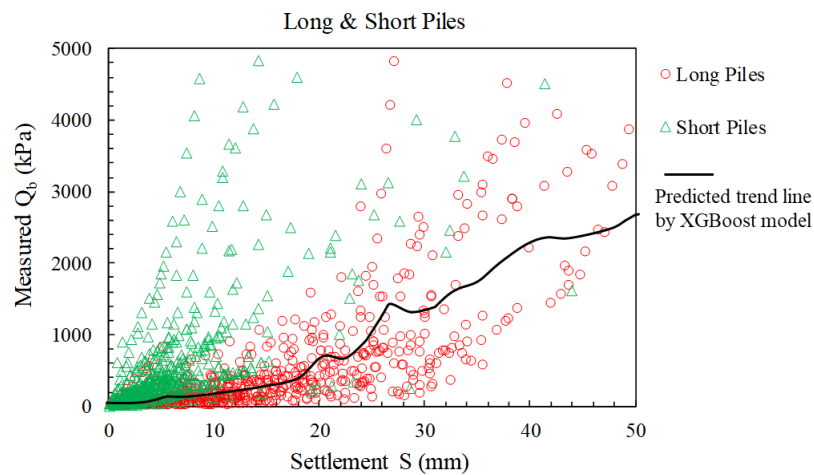


Figure 14. Comparison of trend line given by ML (XGBoost) model and field test datapoints for short and long piles.

In comparison with past suggestions, as well as practice codes, the current findings have some significant implications. For example, Terzaghi [40] stated that the ultimate load occurs when the pile head movement is about 10% of the pile diameter, but Fellenius (2023) indicated that this is only applicable to small piles with a diameter of around 300 mm, which corresponds to the threshold of pile head displacement approximating to 30 mm. On the other hand, according to the National Code for Design of Building Foundation [41] (GB 50007 2011), China, the vertical ultimate bearing capacity of piles is determined based

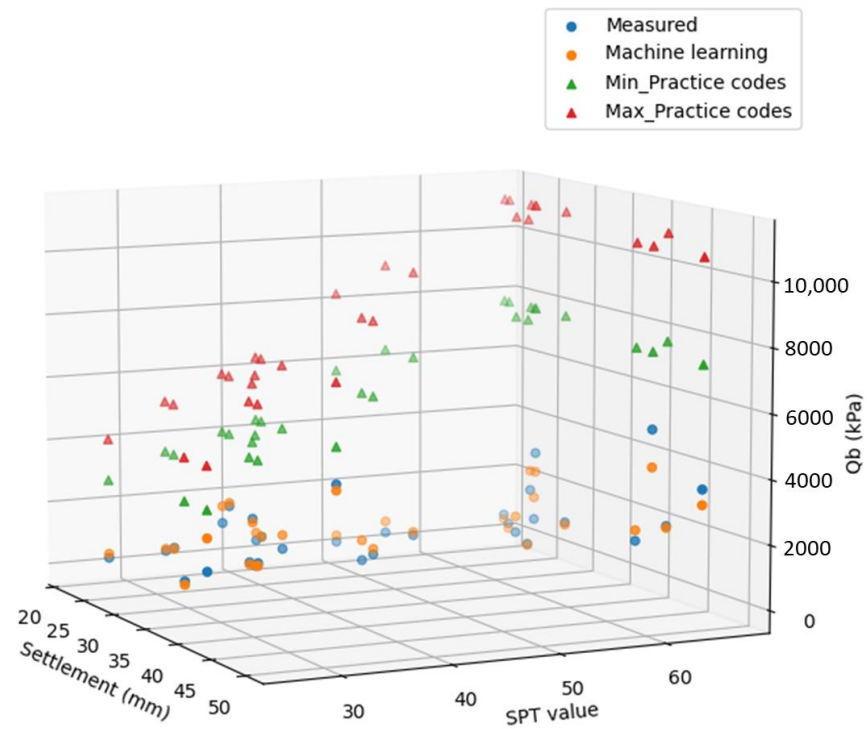
on the load–settlement curves. When the curve does not indicate significant change in the shape, the ultimate load is taken at the pile head settlement of 40 mm. If the pile length is greater than 40 m, the elastic deformation of pile body (pile compression) should be considered, in addition to the head total settlement, and the ultimate bearing capacity can occur when the pile head settlement >40 mm and may reach 60 mm–80 mm. The current findings corroborate this practice as the results (Figures 6 and 13) indicate that, for super-large and long piles (>60 m), the base resistance can account for approximately 25% to 35% of the total ultimate bearing capacity of piles, corresponding to the settlement in the range from 60 mm to 80 mm (>0.1% of the pile length).

Various efforts have been made to employ SPT values (N) for calculating the bearing capacity of pile foundations [42–44], many of which have in fact been adopted widely across various practical design codes and guidelines, such as ASHTO 2010, Vietnamese and Japanese National Standards, among others [39,45] (AASHTO Specifications 2010; TCVN 10304 2014). The most common formula to estimate the unit base resistance (i.e., end-bearing capacity) can be written as [1]

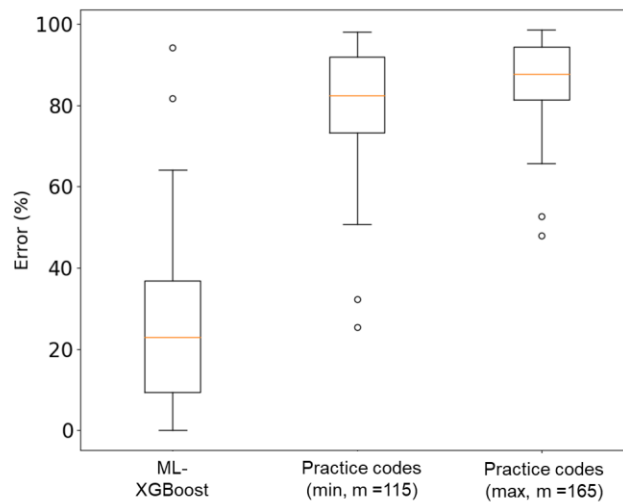
$$Q_b = mN_{SPT} \quad (8)$$

where m is the coefficient changing with different soil and pile types; N_{SPT} is the SPT values of base soil, which can be either the pure or corrected blow counts (N) depending on different standards and requirements. For example, Meyerhof (1976) [42] suggested $m = 120$ (kPa) for bored piles and 400 for driven piles, Karkee et al. (1998) [41] uses $m = 155$ for nodular piles, whereas others further classified m values in different soils. The value of m in sandy soils is often suggested to be 1.5 to 3 times larger than that in clayey soils, e.g., Decourt (1995) [46] proposed m from 115 to 165 for sandy silt to sands, and 80 to 100 for clayey soils in non-displacement piles. In fact, there is a severe lack of practical guidelines on the assessment of the base resistance with respect to different degrees of pile settlement. The Egyptian Code (ECP202/4 2005) [47] is one of very few that considers pile settlement in the calculation of base resistance; however, this oversimplified method, i.e., fixing Q_b with certain magnitudes of settlement, can certainly result in significant errors in prediction.

Figure 15 compares the measured (real) base resistance Q_b in comparison with those predicted by machine learning (XGBoost) and practice codes. In this comparison, the method shown in Equation (8), where m varies from 115 to 165 (min and max, respectively), is adopted as the representative for practice codes. It is important to note that the results are shown in correlation with both settlement S and SPT, which are the two primary parameters used to estimate base resistance. The results indicate a good agreement between the measured and ML (XGBoost)-predicted Q_b , whereas the practice codes yield considerable deviations. Figure 15a shows that the Q_b predicted by the ML method is very close to the measured data (orange and blue dots) across a wide range of settlement and SPT. While the mean prediction error is only about 25% using the machine learning (XGBoost) method, this error exceeds 80% in the cases of practice codes. The results also show that using $m > 150$ in practical design can significantly overestimate the end bearing capacity of piles in sandy soil (the prediction error > 90%). It is noteworthy that the measured Q_b at $S > 20$ mm was considered in this analysis, which enabled the values at ultimate failure to be included.



(a)



(b)

Figure 15. Comparison of machine learning-based predictions incorporating the influence of settlement, and conventional practice methods: (a) 3D distribution of Q_b in relation to S and SPT; and (b) percentage error of prediction.

5. Conclusions

This paper improved our understanding of the influence that settlement (pile head displacement S) can have on the mobilized base resistance (Q_b) of long to super-long piles (i.e., L from 60 to 90 m) through a series of static load test data and machine learning (ML) assessments. Two robust ML algorithms, i.e., the XGBoost and Random Forest (RF), were adopted for model training based on the collected field data, followed by various post-analyses using advanced techniques, such as SHAP, partial dependence plot (PDP) and individual conditional expectation (ICE). Salient findings can be summarized as follows:

1. The field data showed that super-long piles ($L > 60$ m) had very different response to rising settlement (pile head displacement) compared to short and medium piles ($L < 35$ m). While short/medium piles can reach 80% of their ultimate bearing capacity with 50–55% contribution from the base resistance at a settlement threshold S of 10–20 mm (equivalent to 0.015–0.03% of the pile's length), long piles only reached this stage when $S > 40$ –50 mm (>0.08 –0.1% of the pile's length). with the largest contribution at around 20–25% from the base resistance.
2. Settlement was found as the principle key factor affecting behaviour of the base resistance. When settlement increases, it causes compression of the soil underneath the pile toe that resists the applied load. However, when the pile becomes longer, the settlement must propagate, not only through the pile compression, but also the complex load transfer along the pile length, thus reducing its influence on the base resistance. This was reflected through the substantially smaller slope and lower magnitude of the Q_b – S curves in the long piles obtained through in-situ load tests.
3. Empirical equations including the modified hyperbolic formula were proposed for estimating the base resistance of long piles ($L > 60$ m) with acceptable accuracy. This method considers the initial settlement (i.e., approximately 20 mm) induced by pile compression, thus enabling the pile head displacement (surface settlement instead of the displacement of pile tip in conventional formulas) to be used properly.
4. Machine learning (ML) techniques, specifically the XGBoost and RF algorithms, were proved to be effective, not only to predict the base resistance, but also to evaluate the influence that various factors can have on the behaviour of base resistance of piles. Based on the developed model, the SHAP analysis was implemented, and its results further confirmed the predominant impact of settlement on the response of base resistance. More importantly, the settlement-dependent plots of Q_b were successfully created through PDP and ICE techniques, quantitatively presenting how dominantly settlement governed the development of base resistance.

Despite the above achievements, the current study could only address long and very long piles ($L > 40$ m) installed in the soft soil of the Mekong Delta. A larger database that incorporates wider contexts for pile foundations is required to further improve the model. Moreover, other advanced algorithms from machine learning can be used to yield greater benefits to the practical design of deep foundations.

Author Contributions: Conceptualization: T.T.N.; methodology: T.T.N., V.D.L. and T.Q.H.; software: V.D.L.; validation, V.D.L. and T.Q.H.; formal analysis: T.T.N., V.D.L. and T.Q.H.; investigation, V.D.L. and T.Q.H.; resources: T.Q.H.; data curation: V.D.L. and T.Q.H.; writing—original draft preparation: T.T.N. and V.D.L.; writing—review and editing: T.T.N., V.D.L. and N.H.T.N.; supervision: T.T.N.; project administration: T.T.N. All authors have read and agreed to the published version of the manuscript.

Funding: This research received no external funding.

Data Availability Statement: The original data presented in the study are openly available in: <https://zenodo.org/records/11029735>. These data were collected by the authors including 86 static pile load tests on long to very long piles across 37 real-life projects.

Acknowledgments: The field investigation and data collection were supported by a great number of local civil/geotechnical contractors and consultants in Vietnam, such as Hoa Binh Construction Group, FECON South JSC, (FECON Corporation), Bachy Soletanche VN, among others.

Conflicts of Interest: The authors declare no conflicts of interest.

References

1. Fellenius, B.H. Basic of Foundation Design. 2023. Available online: <https://www.fellenius.net/papers/428%20The%20Red%20Book,%20Basics%20of%20Foundation%20Design%202023.pdf> (accessed on 30 March 2024).
2. Galvín, P.; Romero, A.; Solís, M.; Domínguez, J. Dynamic characterisation of wind turbine towers account for a monopile foundation and different soil conditions. *Struct. Infrastruct. Eng.* **2017**, *13*, 942–954. [CrossRef]

3. Nguyen, B.-P.; Nguyen, T.T.; Nguyen, T.H.Y.; Tran, T.-D. Performance of Composite PVD-SC Column Foundation under Embankment through Plane-Strain Numerical Analysis. *Int. J. Geomech.* **2022**, *22*, 04022155. [[CrossRef](#)]
4. Kalauni, H.K.; Masud, N.B.; Ng, K.; Wulff, S.S. Improved Wave Equation Analysis for Piles in Soil-Based Intermediate Geomaterials with LRFD Recommendations and Economic Impact Assessment. *Geotechnics* **2024**, *4*, 362–381. [[CrossRef](#)]
5. Zucca, M.; Franchi, A.; Crespi, P.; Longarini, N.; Ronca, P. The new foundation system for the transept reconstruction of the Basilica di Collemaggio. In Proceedings of the 10th International Masonry Conference, IMC, Milan, Italy, 9–11 July 2018.
6. Hirayama, H. Load-Settlement Analysis for Bored Piles Using Hyperbolic Transfer Functions. *Soils Found.* **1990**, *30*, 55–64. [[CrossRef](#)]
7. Lee, J.H.; Salgado, R. Determination of Pile Base Resistance in Sands. *J. Geotech. Geoenviron. Eng.* **1999**, *125*, 673–683. [[CrossRef](#)]
8. Poulos, H.G. Pile behaviour—Theory and application. *Géotechnique* **1989**, *39*, 365–415. [[CrossRef](#)]
9. Huynh, T.Q.; Nguyen, T.T.; Nguyen, H. Base resistance of super-large and long piles in soft soil: Performance of artificial neural network model and field implications. *Acta Geotech.* **2023**, *18*, 2755–2775. [[CrossRef](#)]
10. Giao, P.H.; Dung, N.T.; Long, P.V. An integrated geotechnical–geophysical investigation of soft clay at a coastal site in the Mekong Delta for oil and gas infrastructure development. *Can. Geotech. J.* **2008**, *45*, 1514–1524. [[CrossRef](#)]
11. Bohn, C.; dos Santos, A.L.; Frank, R. Development of Axial Pile Load Transfer Curves Based on Instrumented Load Tests. *J. Geotech. Geoenviron. Eng.* **2017**, *143*, 04016081. [[CrossRef](#)]
12. Sharo, A.; Al-Shorman, B.; Baker, M.B.; Nusier, O.; Alawneh, A. New approach for predicting the load-displacement curve of axially loaded piles in sand. *Case Stud. Constr. Mater.* **2022**, *17*, e01674. [[CrossRef](#)]
13. Ho, H.M.; Malik, A.A.; Kuwano, J.; Rashid, H.M.A. Influence of helix bending deflection on the load transfer mechanism of screw piles in sand: Experimental and numerical investigations. *Soils Found.* **2021**, *61*, 874–885. [[CrossRef](#)]
14. Chen, H.; Li, L.; Li, J.; Sun, D. A rigorous elastoplastic load-transfer model for axially loaded pile installed in saturated modified Cam-clay soils. *Acta Geotech.* **2022**, *17*, 635–651. [[CrossRef](#)]
15. Xiao, K.; Guo, S.; Wen, J.; Han, J.; Yang, X. Three-Stage Analysis Method for Calculating the Settlement of Large-Diameter Extralong Piles. *Int. J. Geomech.* **2023**, *23*, 04023001. [[CrossRef](#)]
16. Bai, X.; Liu, X.; Zhang, M.; Wang, Y.; Yan, N. Ultimate Load Tests on Bearing Behavior of Large-Diameter Bored Piles in Weathered Rock Foundation. *Adv. Civ. Eng.* **2020**, *2020*, 8821428. [[CrossRef](#)]
17. Li, L.; Li, J.; Wang, Y.; Gong, W. Analysis of nonlinear load-displacement behaviour of pile groups in clay considering installation effects. *Soils Found.* **2020**, *60*, 752–766. [[CrossRef](#)]
18. Zhang, Q.-Q.; Zhang, Z.-M. A simplified nonlinear approach for single pile settlement analysis. *Can. Geotech. J.* **2012**, *49*, 1256–1266. [[CrossRef](#)]
19. Dai, G.; Salgado, R.; Gong, W.; Zhang, Y. Load tests on full-scale bored pile groups. *Can. Geotech. J.* **2012**, *49*, 1293–1308. [[CrossRef](#)]
20. Cao, M.-T.; Nguyen, N.-M.; Wang, W.-C. Using an evolutionary heterogeneous ensemble of artificial neural network and multivariate adaptive regression splines to predict bearing capacity in axial piles. *Eng. Struct.* **2022**, *268*, 114769. [[CrossRef](#)]
21. Nguyen, T.; Ly, D.K.; Huynh, T.Q.; Nguyen, T.T. Soft computing for determining base resistance of super-long piles in soft soil: A coupled SPBO-XGBoost approach. *Comput. Geotech.* **2023**, *162*, 105707. [[CrossRef](#)]
22. Won, J.; Tutumluer, E.; Byun, Y.-H. Predicting permanent strain accumulation of unbound aggregates using machine learning algorithms. *Transp. Geotech.* **2023**, *42*, 101060. [[CrossRef](#)]
23. Baghbani, A.; Choudhury, T.; Costa, S.; Reiner, J. Application of artificial intelligence in geotechnical engineering: A state-of-the-art review. *Earth-Sci. Rev.* **2022**, *228*, 103991. [[CrossRef](#)]
24. Nguyen, T.T.; Huynh, T.Q.; Khabbaz, H.; Le Nguyen, K. Machine learning aided prediction of pile behaviour: The role of data quality. In *Proceedings of the 5th International Conference on Geotechnics for Sustainable Infrastructure Development (GEOTEC HANOI)*; Springer: Hanoi, Vietnam, 2023.
25. Kardani, N.; Zhou, A.; Nazem, M.; Shen, S.-L. Estimation of Bearing Capacity of Piles in Cohesionless Soil Using Optimised Machine Learning Approaches. *Geotech. Geol. Eng.* **2020**, *38*, 2271–2291. [[CrossRef](#)]
26. Nejad, F.P.; Jaksa, M.B. Load-settlement behavior modeling of single piles using artificial neural networks and CPT data. *Comput. Geotech.* **2017**, *89*, 9–21. [[CrossRef](#)]
27. Shahin, M.A. Load-Settlement Modeling of Axially Loaded Drilled Shafts Using CPT-Based Recurrent Neural Networks. *Int. J. Geomech.* **2014**, *14*, 06014012. [[CrossRef](#)]
28. Alkroosh, I.S.; Bahadori, M.; Nikraz, H.; Bahadori, A. Regressive approach for predicting bearing capacity of bored piles from cone penetration test data. *J. Rock Mech. Geotech. Eng.* **2015**, *7*, 584–592. [[CrossRef](#)]
29. Liu, X.; Bai, X.; Zhang, M.; Wang, Y.; Sang, S.; Yan, N. Load-Bearing Characteristics of Large-Diameter Rock-Socketed Piles Based on Ultimate Load Tests. *Adv. Mater. Sci. Eng.* **2020**, *2020*, 6075607. [[CrossRef](#)]
30. Al-Atroush, M.E.; Hefny, A.; Zaghloul, Y.; Sorour, T. Behavior of a Large Diameter Bored Pile in Drained and Undrained Conditions: Comparative Analysis. *Geosciences* **2020**, *10*, 261. [[CrossRef](#)]
31. Ardalan, H.; Eslami, A.; Nariman-Zadeh, N. Piles shaft capacity from CPT and CPTu data by polynomial neural networks and genetic algorithms. *Comput. Geotech.* **2009**, *36*, 616–625. [[CrossRef](#)]
32. Mylonakis, G. Winkler modulus for axially loaded piles. *Géotechnique* **2001**, *51*, 455–461. [[CrossRef](#)]
33. Eid, M.; Hefny, A.; Sorour, T.; Zagh, Y. Full-scale well instrumented large diameter bored pile load test in multi layered soil: A case study of damietta port new grain silos project. *Int. J. Curr. Eng. Technol* **2018**, *8*, 85–98. [[CrossRef](#)]

34. Chen, T.; Guestrin, C. XGBoost: A Scalable Tree Boosting System. In Proceedings of the 22nd ACM SIGKDD International Conference on Knowledge Discovery and Data Mining, San Francisco, CA, USA, 13–17 August 2016; pp. 785–794.
35. Lundberg, S.M.; Lee, S.-I. A unified approach to interpreting model predictions. In Proceedings of the 31st International Conference on Neural Information Processing Systems, Long Beach, CA, USA, 4–9 December 2017; Curran Associates Inc.: Long Beach, CA, USA, 2017; pp. 4768–4777.
36. Molnar, C. Interpretable Machine Learning—A Guide for Making Black Box Models Explainable. 2023. Available online: <https://christophm.github.io/interpretable-ml-book/> (accessed on 30 March 2024).
37. Rodríguez-Pérez, R.; Bajorath, J. Interpretation of machine learning models using shapley values: Application to compound potency and multi-target activity predictions. *J. Comput. Aided Mol. Des.* **2020**, *34*, 1013–1026. [[CrossRef](#)] [[PubMed](#)]
38. Le Nguyen, K.; Trinh, H.T.; Nguyen, T.T.; Nguyen, D.N. Comparative study on the performance of different machine learning techniques to predict the shear strength of RC deep beams: Model selection and industry implications. *Expert Syst. Appl.* **2023**, *230*, 120649. [[CrossRef](#)]
39. *AASHTO Specifications, LRFD Bridge Design Specification*; American Association of State Highway Officials: Washington, DC, USA, 2010.
40. Terzaghi, K. *Discussion of the Progress Report of the Committee on the Bearing Value of Pile Foundations*; ASCE: Reston, VA, USA, 1942.
41. *GB 50007*; Code for Design of Building Foundation, in National Standard of The People’s Republic of China. China Architecture and Building Press: Beijing, China, 2011.
42. Karkee, B.M.; Kanai, S.; Horiguchi, T. Quality assurance in bored PHC nodular piles through control of design capacity based on loading test data. In Proceedings of the 7th International Conference & Exhibition on Piling and Deep Foundations, Vienna, Austria, 15–17 June 1998.
43. Meyerhof, G.G. Bearing Capacity and Settlement of Pile Foundations. *J. Geotech. Eng. Div.* **1976**, *102*, 197–228. [[CrossRef](#)]
44. Reese, L.C.; O’Neill, M.W. *Drilled Shafts: Construction and Design*; FHWA: Washington, DC, USA, 1988; Publication No. HI-88-042.
45. *TCVN 10304*; Pile Foundation-Design Standard. Vietnam National Standard. Ministry of Science and Technology: Ha Noi, Vietnam, 2014.
46. Decourt, L. Prediction of load-settlement relationships for foundations on the basis of the SPT. In Proceedings of the Conference in Honor of Leonardo Zeevaert, Mexico City, Mexico, 28 October–6 November 1995.
47. *ECP202/4*; Egyptian Code for Soil Mechanics–Design and Construction of Foundations, Part 4. Deep Foundations: Giza, Egypt, 2005.

Disclaimer/Publisher’s Note: The statements, opinions and data contained in all publications are solely those of the individual author(s) and contributor(s) and not of MDPI and/or the editor(s). MDPI and/or the editor(s) disclaim responsibility for any injury to people or property resulting from any ideas, methods, instructions or products referred to in the content.